Impairment Analysis of WDM-PON Based on Low-Cost Tunable Lasers

Christoph Wagner, Michael H. Eiselt, *Senior Member, IEEE, Fellow, OSA*, Mirko Lawin, Shihuan Jim Zou, Klaus Grobe, *Senior Member, IEEE*, Juan José Vegas Olmos, *Senior Member, IEEE*, and Idelfonso Tafur Monroy, *Senior Member, IEEE*

***Abstract*—WDM-PON is considered for next-generation broadband backhaul and radio access networking. Among different implementation choices, we propose to utilize low-cost tunable lasers at the remote sites, together with a centralized wavelength locker. Practical implementations require a transparently added downstream signaling channel and upstream per-channel pilot tones for channel tagging and remote wavelength control. Together with some unavoidable crosstalk effects during tuning, all of these system-related items lead to impairments. To keep penalties below 1 dB, the modulation index of the signaling channel must be kept below 15%. Similar values result for the upstream pilot tones. In order to limit crosstalk, such systems require reduced launch power during wavelength tuning and can cover up to 40 km differential reach. These results confirm that WDM-PON based on low-cost lasers is a technically viable approach.**

***Index Terms*—Linear impairments, management channel, pilot tone, tunable laser, WDM-PON.**

I. Introduction

MOBILE bandwidths are increasing, as highlighted by Cisco, which forecasts a growth of 53% per year [1]. LTE-Advanced supports this increase in demand on the air interface, leading to a related traffic increase in the radio access network (RAN). In addition, the demand by network operators to consolidate and centralize network functions has led to a separation of radio frequency (RF) signal generation and processing in centralized baseband units and RF-band / baseband conversion in remote radio heads. The related transmission is commonly called *fronthaul* and further increases bandwidth demand in the RAN [2].

Fronthaul requires protocol transparency since in most cases, it is based on protocols like the common public radio interface (CPRI) [3]. In certain radio applications, it also has a stringent latency requirement. This includes emerging wireless techniques like beamforming or cooperative multipoint. In addition, the migration from backhaul to fronthaul (or, in the 5G context, something in between [4]) is ongoing. Since mobile backhaul is based on Ethernet, next-generation RAN must be compatible with any of the related protocols.

A possible cost-effective solution to satisfy high bandwidth demands as well as protocol transparency are multi-wavelength passive optical network (PON) systems. There, two types of optical distribution networks (ODNs) can be distinguished. First, power-split ODNs are based on wavelength-agnostic power splitters, broadcasting all wavelengths to each optical networking unit (ONU). They are employed in PON systems based on time-division multiple access (TDMA) like G-PON [5] or NG-PON2 [6]. Second, a wavelength-filtered ODN, on the other hand, uses wavelength-division multiplexing (WDM) filters for routing (pairs or groups of) wavelengths to the respective clients.

WDM-PON can support high levels of scalability, transparency and reach. The latter can be increased with optional reach extenders (i.e., optical amplification). For operational reasons, the ONUs in the WDM-PON must use wavelength-agnostic transmitters [7], meaning that the wavelength of an ONU does not need to be known a priori. Wavelength-agnosticism can be achieved by either seeded reflective transmitters or tunable lasers. Given the facts of high bandwidth$\times$reach products and higher tolerance to reflections, this paper focuses on tunable low-cost diode lasers [8], [9].

International Telecommunication Union-telecommunication standardization sector (ITU-T) study group 15, question 6 (Q6), is working on the standardization of such tunable-laser-based WDM-PON systems in the draft Recommendation G.metro. Proposals currently discussed in Q6 include the use of upstream pilot tones (PT) for wavelength tagging and control, and the use of a downstream communications channel that is transparently attached to all individual wavelengths. In NG-PON2, a similar signaling channel is defined for the point-to-point WDM overlay system. It is called auxiliary management and communications channel (AMCC) [10].

In this paper, we present the first thorough analysis of the performance of WDM-PON systems using an AMCC in the downstream and PTs in the upstream, considering the major related impairments.

The remainder of the paper is organized as follows:

Section II gives an overview of the tunable laser-based WDM-PON concept. Section III describes the requirements and impairments in the downstream channel. Section IV analyzes the performance losses in the upstream due to the PTs and pro-

Manuscript received July 25, 2016; revised September 30, 2016; accepted October 9, 2016. Date of publication October 11, 2016; date of current version November 1, 2016. This work was supported in part by the Marie Curie Initial Training Network project ABACUS, the European Community's Seventh Framework Program (FP7/2007-2013) under Grant 317762 (ICT-COMBO), and Horizon 2020 under Grant 671551 (5G-Xhaul).

C. Wagner is with the Department of Photonics Engineering, Technical University of Denmark, 2800 Kgs. Lyngby, Denmark, and also with the ADVA Optical Networking SE, 98617 Meiningen, Germany (e-mail: cwagner@advaoptical.com).

M. H. Eiselt, M. Lawin, and S. J. Zou are with ADVA Optical Networking SE, 98617 Meiningen, Germany (e-mail: meiselt@advaoptical.com; MLawin@advaoptical.com; jzou@advaoptical.com).

K. Grobe is with ADVA Optical Networking SE, 82152 Martinsried, Germany (e-mail: kgrobe@advaoptical.com).

J. J. Vegas Olmos and I. Tafur Monroy are with DTU Fotonik, 2800 Kgs. Lyngby, Denmark (e-mail: jjvegasolmos@gmail.com; idtm@fotonik.dtu.dk).

Color versions of one or more of the figures in this paper are available online at http://ieeexplore.ieee.org.

Digital Object Identifier 10.1109/JLT.2016.2617118

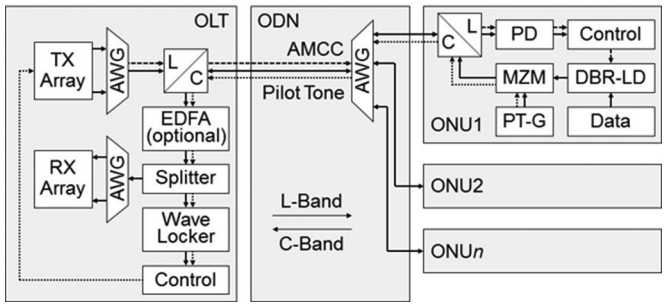

Fig. 1. WDM-PON system based on low-cost tunable lasers. TX: transmitter, RX: receiver, AWG: arrayed waveguide grating, PD: photodetector, MZM: Mach–Zehnder modulator, PT-G: pilot-tone generator, DBR-LD: distributed Bragg reflector-laser diode.

TABLE I
MEAN TIMES BETWEEN DROPPED AND ERRED MESSAGES

Message channel BER	Mean time between dropped messages[a]	Mean time between erred messages[b]
10^{-6}	3.6 days	893 years
2.10^{-6}	22 h	125 years
5.10^{-6}	3.5 h	7.8 years
10^{-5}	53 min	1 year
2.10^{-5}	13 min	44 days
5.10^{-5}	2 min	3 days
10^{-4}	32 sec	8.6 h

[a]Based on the probability of two-bit errors in a message plus half the probability of three-bit errors in a message.
[b]Based on half the probability of three-bit errors in a message plus probability of four or more bit errors in a message.

poses mitigation techniques. In Section V, we analyze the ONU start-up phase and discuss anti-crosstalk mitigation. Section VI concludes the paper.

II. System Concept

In laser-based WDM-PON systems, preferably low-cost tunable lasers are used for the ONUs. For cost reduction, these lasers possibly lack an own dedicated wave locker, and they may not be fully calibrated (since per-sample calibration is costly) [8]. Then, laser monitoring and control, which is still required, can be provided in the system context by a centralized wave locker in the OLT. This needs to be supported by suitable downstream signaling and upstream channel tagging. The latter can be done with PTs [11], [12]. Fig. 1 shows a possible system setup for such an approach.

In the WDM-PON optical line termination (OLT), fixed or tunable lasers might be used. Tunable lasers would reduce spare stock, while fixed lasers possibly are cheaper. A further option would be the use of transceiver arrays with fixed wavelengths.

A low-bit-rate signaling channel can be implemented in the overhead of several communication protocols. However, this approach requires protocol termination in the ONU, which would severely limit the applications of the WDM-PON system due to protocol opaqueness. Therefore, the preferred solution is an AMCC modulated transparently onto each optical channel.

For start-up of a new ONU, the OLT sends the PT frequency and target wavelength via the AMCC to the ONU. During start-up, the ONU transmitter modulates its PT with the assigned frequency onto CW light. The ONU then starts tuning its wavelength without data modulation. As soon as the OLT detects the ONU pilot-tone frequency in one of the receivers, it informs the ONU via the AMCC. Having reached the correct channel, upstream data transmission begins, during which the ONU modulates the PT onto the payload data and continuous wavelength fine-tuning is performed based on the wavelocker in the OLT and control information sent via the AMCC. Wavelength tuning algorithms are proposed in [13]–[15].

AMCC and PTs lead to certain penalties on the payload, and vice versa. Amplifiers in the OLT can influence the PTs as well. Finally, lasers without full calibration can lead to crosstalk in already established upstream channels during start-up. All these effects are analyzed in the following sections.

For ONU monitoring and management, an AMCC can also be used in the upstream. This is done, e.g., in NG-PON2 and is also intended to be included in G.metro.

A similar tuning process can be used for tunable OLT lasers with little extra efforts.

III. Downstream Analysis

The AMCC can be implemented via PTs with amplitude-shift keying, phase-shift keying, or frequency-shift keying modulation. Direct envelope modulation of digital data onto the optical channel is an efficient alternative in terms of effort and cost. It needs a certain modulation depth to achieve sufficient bit-error rate (BER). On the other hand, it reduces the eye opening and leads to a power penalty of the payload.

In the following subsections, we evaluate the implementation details of the AMCC, and the impairments caused by data payload onto the AMCC and vice versa.

A. AMCC Requirements

An AMCC transports control commands for tuning the ONU laser. To avoid wrong tuning of the ONU transmitter, errors in the AMCC must be corrected or at least detected in order to discard the message. In Q6, an AMCC with 64-bit messages and extended Hamming code has been discussed. Seven parity bits are added to 57 payload bits, resulting in a Hamming distance of 4. As a result, single errors can be corrected, and double and some triple errors can be detected and the message can be discarded.

Assuming 64-bit messages and an AMCC bit rate of 100 kbps, the mean time between discarded and erroneous messages are calculated as shown in Table I.

Dropped messages only cause delay in the tuning process because the ONU waits for the next message. Erred messages, in contrast, can lead to mistuning and should be avoided.

A BER of $2 \cdot 10^{-6}$ at 100 kbps leads to some triple errors or more every $\sim$125 years, which cannot be detected leading to erred and un-discarded messages.

B. AMCC Performance

The measurement setup to evaluate the AMCC performance is shown in Fig. 2.

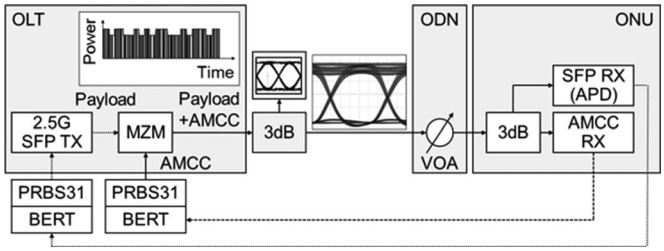

Fig. 2. Measurement setup for AMCC sensitivity evaluation under the influence of the payload and vice versa. The eye-diagram inset shows a 2.5-Gbps payload signal with a 100-kbps NRZ envelope modulation.

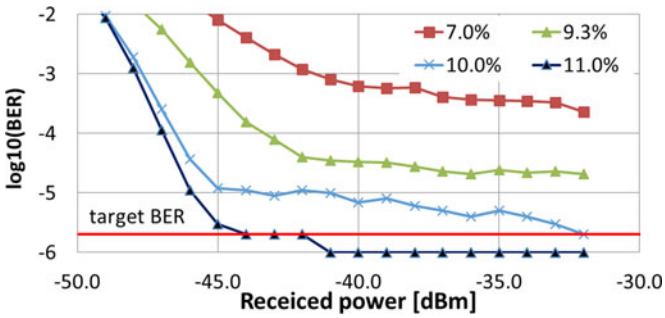

Fig. 3. Bit error rate vs. received power of an envelope modulated 100-kbps message channel. The modulation depth varied from 7% to 11%.

An optical signal at 2.5 Gbps carrying a pseudo-random bit sequence (PRBS) of length 2^{31}-1 (PRBS-31) is amplitude-modulated with the AMCC data using a Mach-Zehnder modulator (MZM). The combined signal is split and one portion is used to measure the eye diagram to evaluate the AMCC modulation depth. The second portion is split again to measure the BER of the payload and of the AMCC as a function of the received power. The AMCC modulation depth is defined as the peak-to-peak power variation of the payload "one" rail divided by the maximum payload "one" rail power.

The AMCC sensitivity was measured as a function of the received power for 100 kbps non-return-to-zero (NRZ) modulation and for various modulation depths under the impact of a 2.5-Gbps PRBS-31 payload. The data rate 2.5 Gbps with PRBS-31 was chosen as the payload with lowest expected frequency content. While GbE as well as low CPRI rates are 8B/10B coded, the uncoded 2.5 Gbps modulation is the most stressing payload data. We verified that the performance of the AMCC is far better for 10.7-Gbps, PRBS-31 or 1.25-Gbps, PRBS-7 payloads.

Fig. 3 shows the BER of the AMCC for modulation depths between 7% and 11%. For all modulation depths, an error floor is observed. We associate this error floor with the spectral components of the payload falling into the AMCC receiver bandwidth. In other words, the on-off modulation of the payload acts like noise on the AMCC and is increased with increasing power level. Only for higher AMCC modulation depths, the relative noise is reduced.

As described above, a BER of at least $2 \cdot 10^{-6}$ is required to ensure an acceptable performance of the AMCC (red line in Fig. 3). A modulation depth between 10 and 11% is required for this BER, and a received power around −40 dBm is necessary.

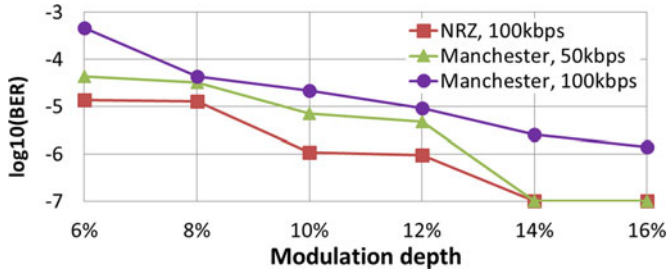

Fig. 4. Error floor as function of the modulation depth at –35 dBm for 100 kbps NRZ encoding compared to 50 kbps and 100 kbps Manchester encoding.

The NRZ format is not fully optimum for the AMCC due to a necessary clock for data recovery. A modulation format including the clock is preferred in terms of cost-efficiency and simplicity. Manchester coding supports clock recovery from the transmitted data. One drawback is the bandwidth demand, which is twice as high as for NRZ. The AMCC error floor for Manchester coding is shown in Fig. 4 as a function of the modulation depth at a received power of −35 dBm.

We transmitted $2 \cdot 10^7$ bits for each data point. BER values of 10^{-7} indicate bit-error-free transmission. 100-kbps NRZ and 50-kbps Manchester-coded signals show similar performance. Both encoding schemes show a BER floor better than 10^{-6} for a modulation depth of 14% and above. The 100-kbps Manchester-encoded AMCC suffers more from the interaction with the payload, as explained above. An error floor of 10^{-6} is not achieved for modulation depths below 16% and therefore, Manchester-encoded 100 kbps AMCC was not evaluated further.

Next, we evaluate the sensitivity of the payload in presence of an AMCC with Manchester and NRZ encoding.

C. AMCC Impact on Payload

Envelope modulation of the AMCC reduces the eye opening of the payload as a function of the modulation depth of the AMCC. An appropriate AMCC performance requires a modulation depth between 10% and 14%, depending on the modulation format and AMCC bitrate.

For evaluation of AMCC impact on payload, the same setup was used as for the AMCC sensitivity measurements, see Fig. 2. The receiver sensitivity was measured for a 2.5-Gbps signal in the presence of an AMCC with 10% and 15% modulation depth. 15% modulation depth was chosen to have some additional safety margin for the AMCC. The BER versus received payload power in presence of an AMCC with 100 kbps NRZ and 50 kbps with Manchester coding is shown in Fig. 5(a) for 10% modulation depth and in Fig. 5(b) for 15%, respectively.

The AMCC impact on the payload only marginally depends on modulation format and data rate. At a payload BER of 10^{-12}, the penalty due to an AMCC with 10% and 15% modulation depth is below ∼0.5 dB and ∼1 dB, respectively.

IV. Upstream Analysis

In this section, we compare two implementations of pilot-tone (PT) envelope modulation and their impact on the payload. We also analyze the impairments on the PT due to an EDFA.

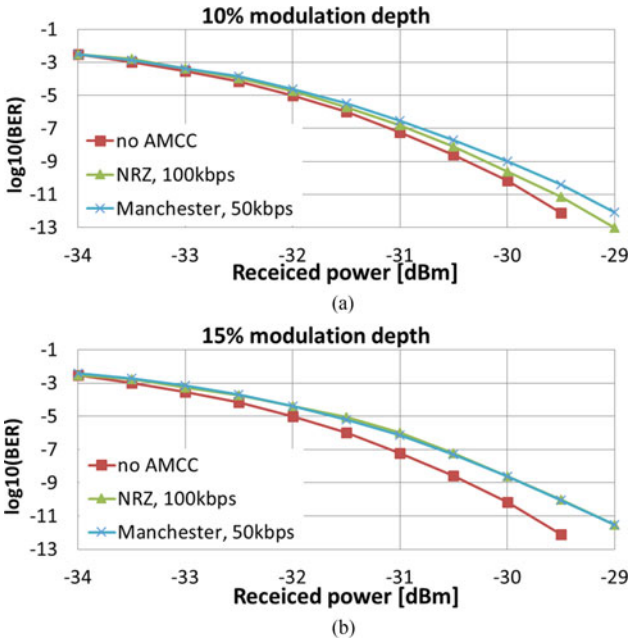

Fig. 5. Bit error rate of the 2.5-Gbps payload channel vs. received power with a) 10% and b) 15% modulation depths of the envelope modulation. "no AMCC" is the case without envelope modulation.

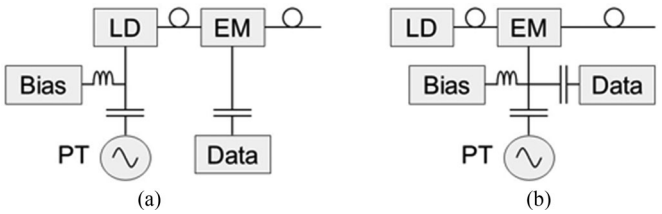

Fig. 6. Pilot tone generation. a) Adding a small sinusoidal current to the laser's bias current, b) dithering of the bias voltage of external modulator.

A. Pilot Tone Generation

In upstream direction, a PT is modulated on each channel for wavelength control at the centralized wavelength locker. Considering low cost implementation, we evaluated two intensity modulation methods shown in Fig. 6.

Multiplicative PT modulation: Fig. 6(a) shows the block diagram for modulating the PT directly on the laser bias current while the payload data *d(t)* are modulated via an external modulator. The resulting power *P(t)* can be formulated as

$$P(t) = \hat{P} \cdot [1 + m \cdot \cos(2\pi f_{\text{tone}} t)] \cdot d(t). \quad (1)$$

$\hat{P}$ is the unmodulated laser output power, f_{tone} the PT frequency, and *m* the modulation index of the PT. The PT modulation depth *m* is defined as

$$m = \frac{P_{\max} - P_{\min}}{P_{\max} + P_{\min}}. \quad (2)$$

$P_{\max}$ and $P_{\min}$ are the maximum and minimum optical power during a mark rail due to superposition with the PT.

In this modulation scheme, the pilot tone is introduced as a multiplier to the data, resulting in a convolution of the PT spectrum with the data spectrum. The same result would be obtained by modulating the PT onto the modulated signal via an external modulator or a VOA.

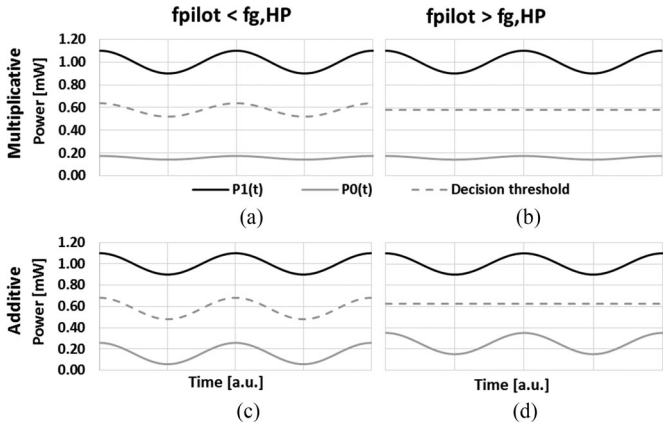

Fig. 7. Time-resolved pilot-tone modulation of mark [P1(t)] (black) and space [P0(t)] (grey). Upper row: multiplicative modulation, bottom row: additive modulation. Left column: PT frequency below lower cut-off frequency $f_{g,\text{HP}}$ (decision threshold (dashed) follows average power), right column: PT frequency above lower cut-off frequency $f_{g,\text{HP}}$ (decision threshold is constant).

Additive PT modulation: Fig. 6(b) shows PT-induced dithering of the bias voltage of an external modulator. Adding the PT to the bias of an external modulator can be expressed as

$$P(t) = \hat{P} \cdot [d(t) + m \cdot \cos(2\pi f_{\text{tone}} t)]. \quad (3)$$

The power spectral density of the PT is linearly added to the data spectrum. This results in an additional line in the data spectrum.

B. Pilot Tone Impact on Data—Simulation

PT modulation causes a power penalty of the data signal. The additive PT modulation has the benefit that the PT can be filtered out when the PT frequency is below the lower cut-off frequency of the payload receiver, which is formed by the AC coupling and the TIA input impedance. Then, the data signal remains undistorted. For multiplicative PT modulation, mixing products of PT and data are present in the whole data spectrum.

Four different situations are shown in Fig. 7. The left column shows the cases for PT frequencies below the lower cut-off frequency of the receiver bandpass caracteristics $f_{g,\text{HP}}$. The slowly varying PT is dropped at the receiver input filter (AC coupling and TIA input impedance), which corresponds to a decision threshold *DT(t)* for the data signal which follows the PT. For PT frequencies exceeding the lower cut-off frequency (right column), the decision threshold does not follow the average signal and remains constant, leading to non-optimum threshold.

Assuming a Gaussian noise distribution with the same variance σ for mark and space, the BER can be calculated by

$$\text{BER}(t) = \frac{1}{2} \cdot \left[\text{erfc}\left(\left| \frac{P1(t) - DT(t)}{\sigma} \right| \right) + \text{erfc}\left(\left| \frac{DT(t) - P0(t)}{\sigma} \right| \right) \right]. \quad (4)$$

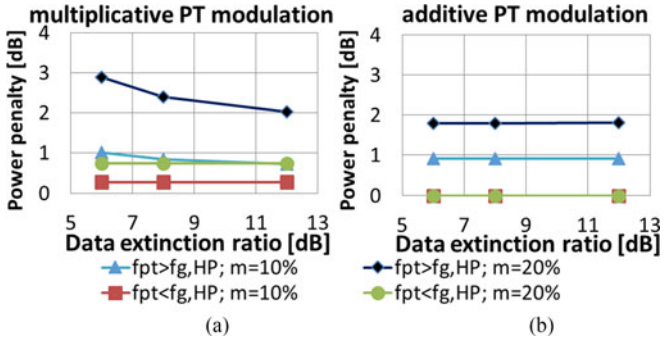

Fig. 8. Power penalty of data signal at BER = 1E-9 as function of the extinction. a) Multiplicative PT modulation, b) additive PT modulation (circle and square curve overlay). m: PT modulation depth; $f_{g,\mathrm{HP}}$: Rx lower cut-off frequency.

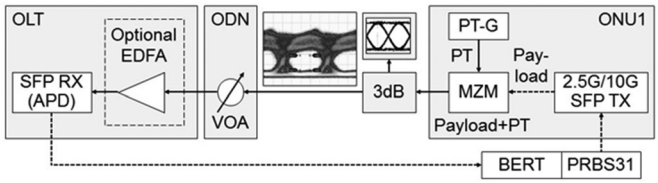

Fig. 9. Measurement setup for power penalty evaluation of a pilot tone on a data signal with multiplicative PT modulation scheme.

By averaging the time-resolved BER over one PT period, the power penalty can be derived, as shown in Fig. 8. For low PT frequencies and additive modulation, the data power penalties are negligible, whereas for multiplicative modulation, a penalty can be observed. For high extinction ratios and high PT frequencies, both modulation schemes result in comparable power penalties.

C. Pilot Tone Impact on Data—Measurements

To verify our theoretical results, we used the multiplicative modulation scheme and measured the power penalty for 2.5-Gbps and 10-Gbps payloads using two different SFPs.

Fig. 9 shows the measurement setup. Signals at data rates of 2.5 Gbps and 10 Gbps were modulated with a PRBS-31. The extinction ratio of the data signal was ∼8 dB for both SFPs. The PT was modulated via an MZM onto the data-modulated optical signal (multiplicative scheme). The optical signal was split into two portions. One portion was sent to an analyzer to monitor the modulation depth of the PT, the second portion was sent to the receiver of the SFP to measure the BER as a function of the received power.

The power penalties for 2.5 Gbps and 10 Gbps are similar as shown in Fig. 10. Far above the lower cut-off frequency, they remain almost constant. For low PT frequencies, a power penalty is still observed. These results are in agreement with the theoretically analyzed power penalties.

PT frequencies below the lower cut-off frequency and modulation depth of 10% lead to a power penalty of ∼0.2 dB. Increasing the PT frequency above the lower cut-off frequency yields a power penalty of ∼1.3 dB.

We conclude that a PT frequency below the lower cut-off frequency keeps the payload power penalty small. Therefore, the lower cut-off frequency of the SFP can be used as an upper bound for the PT frequency. Regarding payload penalty, the PT modulation depth should be 10% or lower. In experiments, the detection of a PT with 10% modulation depth successfully tested. However, the PT detection depends heavily on receiver electronics and were not further evaluated.

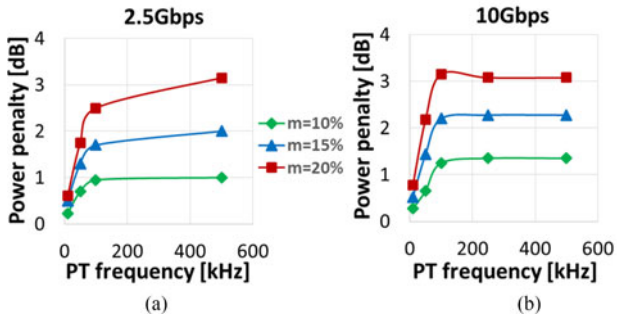

Fig. 10. Measured power penalty of data signal as function of the PT frequency for different modulation depths. Left: 2.5 Gbps, right: 10 Gbps. m: PT modulation depth.

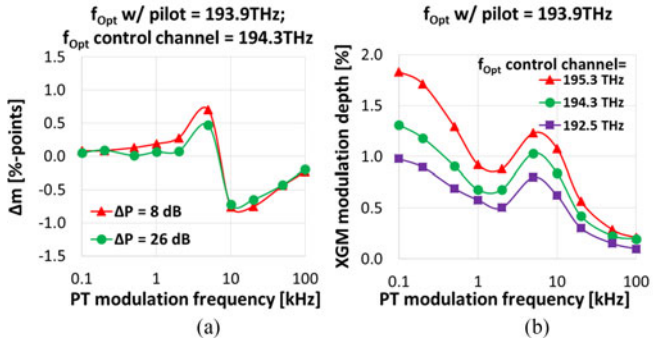

Fig. 11. EDFA impact on pilot tone. a) modulation-depth change Δm, b) XGM.

D. Pilot Tones in Amplified PON Systems

Optical amplification for reach extension should be a possible option. EDFAs at the OLT keep the ODN passive and can extend the reach. However, an EDFA can affect the PT in several aspects. Saturated EDFA carrier dynamics can reduce or cancel the PT modulation. Furthermore, cross gain modulation (XGM) can imprint a PT on all other channels, which would lead to pilot-tone detection in wrong channels. EDFA gain control can partly negate these effects.

The PT was modulated on a tunable laser emitting at 193.9 THz. The pilot-tone modulation depth into the EDFA was set to 20% and was measured again after the EDFA. An unmodulated control channel emitting at 194.3 THz was launched into the EDFA as well. The impact of an EDFA on the modulation depth of the PT is shown in Fig. 11(a). For evaluation of the influence on the modulation depth of the PT, the power difference ΔP between the pilot-tone channel and the unmodulated control channel was varied between 8 dB and 26 dB. This power difference has negligible effect, and the plots almost coincide. Two extrema are visible. At 5 kHz, the PT modulation depth is increased to 20.5% and at 10 kHz, it is reduced to 19.25%. Increasing the PT frequency further, the modulation depth

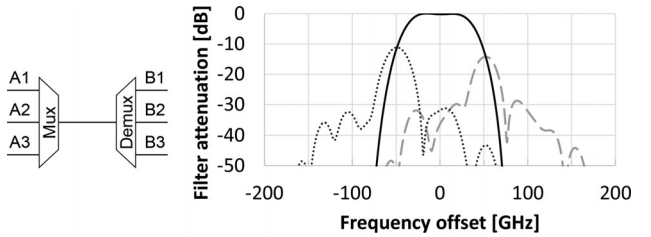

Fig. 12. Filter function of two cascaded 100-GHz AWGs. Solid line: Target channel (A2→B2), dotted and dashed lines: crosstalk, when laser is connected to upper and lower neighboring port of multiplexer filter (A1→B2 or A3→B2).

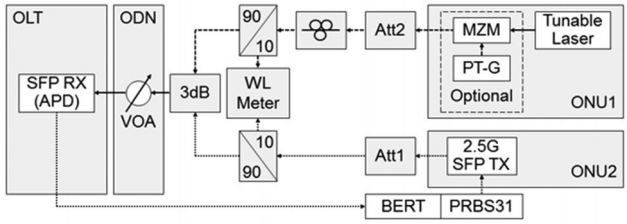

Fig. 13. Measurement setup for coherent and incoherent crosstalk evaluation with and without pilot tone modulation.

approaches its former modulation depth value of 20%. Considering a PT modulation depth margin of ±1%-points leads to no PT-frequency restrictions.

Amplifier XGM can imprint a PT on all other channels and cause ghost tones. XGM versus PT frequency is shown in Fig. 11(b) for different wavelengths of the unmodulated control channel. The power difference was varied as well. However, for clarity, we selected only the power difference with the highest XGM. We observe that the control channels emitting at short wavelengths are most affected by XGM. This is confirmed by other wavelength configurations. This seems reasonable due to the EDFA gain profile, which shows higher gain for shorter wavelengths.

To keep the XGM below 1% would require a lower limit of the PT frequency of 20 kHz.

V. Crosstalk During Start-Up Tuning

So far, we only considered fixed-wavelength or fully calibrated tunable lasers, which can immediately emit on the correct wavelength. Due to the low-cost requirement, the tunable lasers might not be fully calibrated since this is a time-consuming and costly per-sample process. Centralized wavelength locking and related signaling can provide the necessary laser monitoring and control; however, crosstalk can now occur during the tuning process. This happens when a non-sufficiently calibrated laser has to sweep across (parts of) the upstream wavelength band in order to find its correct channel.

In wavelength-filtered WDM-PON, signals outside the target wavelength channel under consideration are suppressed by the WDM filters. However, channel isolation can be reduced toward the edges of filter channels and lead to a considerable crosstalk. For example, in the case of two cascaded flattop AWGs, the provided channel isolation can be as low as 12 dB at half of the channel spacing for neighboring multiplexer ports. This leads to incoherent crosstalk, as shown in Fig. 12.

Channels can differ in launch power and in optical path and insertion losses between the ONUs and the OLT. Reduced channel isolation can have two effects. First, the tuning ONU could be detected misleadingly in the neighbor channel. This can be avoided by assigning different PT labels to each ONU, which are detected by the dedicated OLT receiver. Only if the respective label is detected with an appropriate power level, the ONU surely emits on the correct wavelength channel. Second, during tuning, a strong tuning channel can interfere with weak working channels, leading to incoherent and coherent crosstalk. These crosstalk effects and mitigation examples are discussed in the subsequent paragraphs.

A. Worst-Case Crosstalk Scenario

During the tuning process, coherent and incoherent crosstalk can occur. For coherent crosstalk, the interferer and the working channel have the same nominal wavelength. Coherent crosstalk is suppressed by the *multiplexing* filter by up to 30 dB. Once passed through that filter, the interferer will not be suppressed any further by the demultiplexing filter. At the OLT receiver, the electrical fields of signal and interferer beat. Therefore, highest coherent crosstalk results for co-polarized signals.

In contrast, incoherent crosstalk mainly occurs at half of the channel spacing. Here, multiplexing and demultiplexing filters suppress interferers with reduced channel isolation. Photodiodes detect both, the respective channel and the insufficiently suppressed interferers. According to Fig. 12, interferers might be suppressed by only 12 dB after both filters.

For crosstalk analysis, the launch-power window ΔP of the ONU transmitter is assumed with 4 dB. The maximum differential path loss (DPL) depends on the maximum system reach. We assume fiber loss of 0.275 dB/km, resulting in 22 dB DPL for an 80-km system.

With the values stated above, and assuming worst cases, signal-to-interferer ratio (SIR) of 4 dB and -14 dB results for coherent and incoherent crosstalk, respectively.

B. Experimental Crosstalk Analysis

For crosstalk evaluation, we used the measurement setup shown in Fig. 13. A PRBS-31 signal was generated in SFP at a bit rate of 2.5 Gbps. This signal was then split by a 90/10 splitter. The major portion was sent to the SFP receiver via a 3-dB combiner and a VOA for measuring the BER versus received optical power. The minor portion was sent to a wavelength meter. As interferer, we used a tunable laser. We used two interferer schemes, a DC interferer and an interferer with a low pilot-tone modulation frequency. For the DC interferer, the tunable-laser light was split in another 90/10 splitter. The minor portion was sent to the wavelength meter to determine the frequency offset. The major portion was combined with the SFP signal in the 3-dB coupler. A polarization controller (PC) was used to align the polarization of the interferer for the worst BER. Attenuators (ATT) 1 and 2 were used to adjust the SIR.

For modulation with a low pilot-tone frequency, an MZM was inserted and modulated by a sinusoidal generator with a modulation depth of 10%.

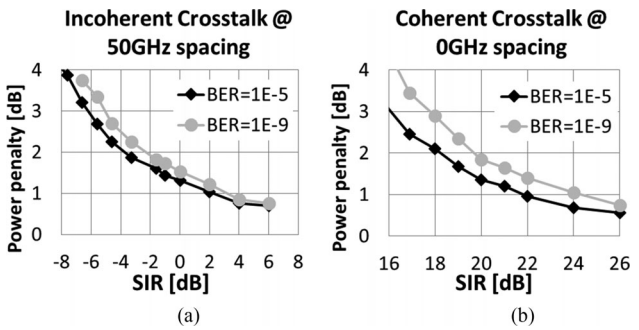

Fig. 14. Penalty measurement for left: incoherent crosstalk ($\Delta f \sim 50$ GHz), and right: coherent crosstalk ($\Delta f \sim 0$ GHz) without pilot tone modulation.

C. Experimental Results

We studied four crosstalk scenarios.

1) Power penalty over SIR for incoherent crosstalk (assuming 100 GHz channel spacing and frequency deviation Δf of 50 GHz).
2) Power penalty over SIR for coherent crosstalk (frequency deviation $\Delta f = 0$ GHz).
3) Power penalty over frequency deviation to measure the spectral crosstalk range and transition from incoherent to coherent crosstalk.
4) Power penalty for a modulated interferer with different pilot-tone frequencies for coherent and incoherent crosstalk.

We assumed a maximum allowed crosstalk penalty of 1 dB.

Fig. 14(a) shows the power penalty for incoherent crosstalk at 50 GHz frequency offset without PT modulation. For a BER of 10^{-9}, the power penalty is below 1 dB for SIR values higher than 3 dB. Therefore, incoherent crosstalk needs to be improved by up to 17 dB, as the worst-case SIR in the system assumed above is -14dB.

Fig. 14(b) depicts the power penalty for coherent crosstalk ($\Delta f = 0$ GHz). For 1 dB penalty, an SIR of $\sim$24 dB is needed. Since worst-case coherent-crosstalk SIR in the system assumed above is 4 dB, the SIR needs to be improved by up to 20 dB.

Finally, the interferer was PT-modulated in the multiplicative scheme with 10% modulation depth, and the PT frequency was varied between 1 Hz and 10 MHz. Negligible additional penalty of $<$0.1 dB was measured for coherent crosstalk with an SIR of 22 dB over the whole frequency range. For incoherent crosstalk, we used an SIR of 0 dB. The additional penalty due to the PT is negligible for PT frequencies $<$10 kHz. For PT frequencies between 10 and 100 kHz, the power penalty rises to 0.25 dB and remains constant for higher PT frequencies. These results confirm the results shown in Section IV.

In a worst case scenario, the coherent and incoherent crosstalk is $\sim$20 dB higher than the required SIR to keep the power penalty below 1 dB. Several techniques can be applied to mitigate crosstalk during tuning, e.g., limiting the differential path loss (DPL), power reduction during tuning, reducing the transmitter launch-power window, polarization control (scrambling), and /or improving the filter channel isolation. We analyzed the aforementioned possibilities and estimate their benefits and drawbacks.

1) Limiting the launch-power window increases the worst case SIR by $\sim$2 dB. This limited benefit must be related to the cost that results from lower laser yield.
2) Introducing polarization scrambling reduces the required SIR by $<$3 dB. The additional cost and system complexity of an additional pol. scrambler surpasses its benefit.
3) Improvement of filter channel isolation is limited as well. Isolation depends on filter technology. Its increase can have associated negative effects on both, filter cost and insertion loss.
4) The most promising mitigation techniques are reduced DPL and power reduction during tuning. To maintain certain DPL, the launch power should be reduced during tuning. For directly modulated lasers, launch-power reduction by 20 dB is challenging without hitting the laser threshold current. We assume that 10 dB power reduction is possible for directly modulated laser. Then, limiting the differential reach to 40 km is sufficient to keep the SIR in an acceptable range.

VI. Conclusion

We report on our approach of a WDM-PON system based on tunable lasers and a centralized wavelocker. We analyzed the impairments in such WDM-PON systems using an AMCC in downstream direction for assigning the PT frequency and target wavelength of the ONU, and PTs in upstream direction used as channel label.

In downstream, AMCC modulation depth of 11 . . . 15% leads to a BER below $2 \cdot 10^{-6}$ for received powers of –40 dBm and higher. Then, erred AMCC messages occur every $\sim$125 years on average, which is regarded sufficient. An AMCC with 100 kbps NRZ or 50 kbps Manchester coding leads to a payload penalty of 1 dB, which is regarded sufficiently low as well.

In upstream, we analyzed the impairments of pilot tones on the payload, and of EDFAs on the pilot tones. A pilot tone with 10% modulation depth leads to $\sim$1.5 dB power penalty for the payload. This is reduced for pilot-tone frequencies below the lower cut-off frequency of the payload receiver. Therefore, the receiver lower cut-off frequency can be used as upper bound for the pilot-tone frequency (e.g., 100 kHz). An optionally added EDFA leads to acceptable effect on the pilot tones. XGM shows a wavelength dependence similar to the gain spectrum of the EDFA. It reduces with increasing pilot-tone frequency and sets a lower frequency limit of 20 kHz for amplified systems. Therefore, also the pilot-tone scheme is feasible, with regard to the related impairments.

Finally, we analyzed crosstalk during ONU start-up, caused by insufficiently calibrated low-cost lasers. The major challenge is high differential reach. Power reduction during tuning and differential reach reduced to 40 km keep the penalty caused by coherent and incoherent crosstalk below 1 dB.

In conclusion, we find that loosely calibrated low-cost lasers, enabled by centralized wave locking, transparent downstream signaling and pilot-tone upstream channel tagging, can be used for WDM-PON with high bandwidth$\times$reach products.

References

[1] T. Cisco, “Cisco visual networking index: Global mobile data traffic forecast update, 2010–2015,” White Paper, 2011.

[2] K. Miyamoto, S. Kuwano, J. Terada, and A. Otaka, "Analysis of mobile fronthaul bandwidth and wireless transmission performance in split-PHY processing architecture," *Opt. Express*, vol. 24, no. 2, pp. 1261–1268, 2016.
[3] Common Public Radio Interface (CPRI), *Interface Specification*, 2013.
[4] D. Muench, "Converged ethernet for next-generation x-haul," presented at the Joint Workshop iCirrus, 5G-XHaul, 5G-Crosshaul projects, EuCNC, Athens, Greece, Jun. 2016
[5] *Gigabit-Capable Passive Optical Networks (GPON): General Characteristics, Amendment 2*, Recommendation ITU-T G.984.1, 2012.
[6] *40-Gigabit-Capable Passive Optical Networks 2 (NG-PON2): Physical Media Dependent (PMD) Layer Specification*, ITU-T G.989.2, 2014.
[7] *40-Gigabit-Capable Passive Optical Networks (NG-PON2): General Requirements*, ITU-T G.989.1, 2013
[8] K. Grobe, M. H. Eiselt, S. Pachnicke, and J.-P. Elbers, "Access networks based on tunable lasers," *J. Lightw. Technol.*, vol. 32, no. 16, pp. 2815–2823, Aug. 2014.
[9] F. Ponzini *et al.*, "Evolution Scenario Toward WDM-PON [Invited]," *IEEE/OSA J. Opt. Commun. Netw.*, vol. 1, no. 4, pp. 25–34, Sep. 2009.
[10] Y. Luo *et al.*, "Physical layer aspects of NG-PON2 standards—Part 2: System design and technology feasibility [Invited]," *IEEE/OSA J. Opt. Commun. Netw.*, vol. 8, no. 1, pp. 43–52, Jan. 2016.
[11] S. Pachnicke *et al.*, "Field demonstration of a tunable WDM-PON system with novel SFP+ modules and centralized wavelength control," in *Proc. Opt. Fiber Commun. Conf. Exhib.*, 2015, vol. 3, pp. 1–3.
[12] J. Zhu *et al.*, "First demonstration of a WDM-PON system using full C-band tunable SFP+ transceiver modules [Invited]," *IEEE/OSA J. Opt. Commun. Netw.*, vol. 7, no. 1, pp. A28–A36, Jan. 2015.
[13] K. Prince *et al.*, "GigaWaM-next-generation WDM-PON enabling gigabit per-user data bandwidth," *J. Lightw. Technol.*, vol. 30, no. 10, pp. 1444–1454, May 2012.
[14] M. Iglesias, R. Rodes, T. T. Pham, and I. T. Monroy, "Real time algorithm temperature compensation in tunable laser/VCSEL based WDM-PON system," in *Proc. Int. Congr. Ultra Mod. Telecommun. Control Syst.*, 2012, pp. 240–242.
[15] S. Pachnicke, M. Roppelt, M. Eiselt, A. Magee, P. Turnbull, and J.-P. Elbers, "Investigation of wavelength control methods for next generation passive optical access networks," in *Proc. 38th Eur. Conf. Exhib. Opt. Commun.*, 2012, pp. 1–3.

Christoph Wagner received the Dipl.-Ing. (FH) degree in telecommunications from the University of Applied Science Berlin (HTW), Berlin, Germany, in 2008, and the M.Sc. degree from the Technical University of Berlin, Berlin, in 2013. In February 2014, he started his Ph.D. study in the Marie-Curie ITN project ABACUS with the Metro-Access group at the Technical University of Denmark, Kgs. Lyngby, Denmark, and developed signal-slicing techniques.

He was a member of the technical staff at the Photonic Components group, Fraunhofer Heinrich Hertz Institute, Berlin, from 2007 to 2013, where he worked on lasers, polymer-based multiplexers, diffractive optical elements, and Mach–Zehnder modulators. In September 2014, he joined the Advanced Technology team at ADVA Optical Networking SE as the Industrial Partner of the Marie-Curie project. At ADVA, he is working on next-generation broadband access technology and is also actively participating in the standardization group Q.6 of ITU-T SG15.

Michael H. Eiselt (M'97–SM'98) received the Dipl.-Ing. degree in electrical engineering from the University of Hannover, Hannover, Germany, in 1989, and the Dr.-Ing. degree from the Technical University of Berlin, Berlin, Germany, in 1994. He was a member of technical staff at Fraunhofer Heinrich Hertz Institute, Berlin, and a Visiting Researcher at AT&T Bell Labs. In 1997, he became a Principal Technical Staff Member at the Lightwave Networks Research Department of AT&T Labs-Research. In 2000, he joined Celion Networks, Tinton Falls, NJ, USA, as a Principal Architect and, in 2005, moved to ADVA Optical Networking SE, Meiningen, Germany, where he is currently the Director of Advanced Technology. He is also actively participating in the standardization group Q.6 of ITU-T SG15. He has authored or coauthored more than 130 journal and conference publications, has coauthored one book, and is an inventor of 40 patents. He is a Fellow of the Optical Society of America, a senior member of the IEEE Photonics Society, and a member of the VDE-ITG. From 2011 to 2014, he was on the OFC technical program subcommittee on "Digital Transmission Systems," chairing the subcommittee for the 2013 conference.

Mirko Lawin received the Dipl.-Ing. (M.Sc. equivalent) degree in optical and electrical engineering from the Technical University of Ilmenau, Ilmenau, Germany, in 1987. He worked in several areas among others in the development of hard discs, optical measurement instruments, self-acting test equipment, mobile-phone electronics, and automotive electronics. He is currently with the Advanced Technology Group (CTO Office), ADVA Optical Networking SE, Meiningen, Germany, where he is working in the field of analog and digital electronics. His current research interests include ultralow-power analog solutions and field-programmable-gate-array–based high-speed electronics for optical networking applications. He is also author or coauthor of a number of scientific publications and holds several patents. He is a member of VDE/ITG.

Shihuan Jim Zou received the B.Eng. degree in communication and information engineering and the M.Sc. degree in electrical circuits and systems from Shanghai University, Shanghai, China, in 2008 and 2011, respectively, and the Ph.D. degree in 2015 from Eindhoven University of Technology, Eindhoven, The Netherlands, where he conducted the research work with the Electro-Optical Communication Group of the COBRA research institute in the area of broadband indoor fiber-wireless networks, which aimed to enhance network flexibility and capacity in order to support future indoor communication needs. Since January 2016, he has been with the Advanced Technology team, ADVA Optical Networking SE, Meiningen, Germany, supporting and participating in various advanced research and prototype development projects related to the next-generation optical access.

Klaus Grobe (M'94–SM'13) received the Dipl.-Ing. and Dr.-Ing. degrees in electrical engineering from Leibniz University, Hannover, Germany, in 1990 and 1998, respectively.

He worked over 20 years in the fields of lightwave guides and WDM. This includes positions as a Technical Staff Member at German and pan-European network operators. In 2000, he joined ADVA Optical Networking SE, Meiningen, Germany, where he is currently the Director of Global Sustainability. He is one of the main authors of *Wavelength Division Multiplexing—A Practical Engineering Guide* (Hoboken, NJ, USA: Wiley, 2014), and authored or coauthored more than 100 technical publications and three book chapters on WDM and PON technologies. His research interests include next-generation broadband access, high-speed WDM transport and sustainability in photonics. He holds 32 (pending) patents.

Dr. Grobe is a member of the German VDE/ITG and ITG Study Group 5.3.3 on Photonic Networks. He served OFC Subcommittee 10 in 2009–2012 and works in FSAN, ITU-T SG15-Q.2, and the QuEST Forum Sustainability Initiative.

Juan José Vegas Olmos (M'03–SM'14) received the B.Sc. and M.Sc. degrees in electronic engineering, the B.A. degree in economics, the M.A. degree in arts, majoring in East Asian studies, and the M.B.A. degree. He also received the Ph.D. degree from Eindhoven University of Technology, Eindhoven, The Netherlands, in 2006. He was further trained at Osaka University as a Japan Society for the Promotion of Science (JSPS) Fellow and subsequently worked as a Senior Researcher at Hitachi Central Research Laboratory, Tokyo, Japan. In 2011, he joined the Technical University of Denmark, Kgs. Lyngby, Denmark, where he has been an Associate Professor at the Department of Photonics Engineering since 2013. He is a JSPS Fellow and a Marie Curie Fellow.

Idelfonso Tafur Monroy (SM'14) graduated from Bonch-Bruevich Institute of Communications, St. Petersburg, Russia, in 1992, where he received the M.Sc. degree in multichannel telecommunications. In 1996, he received the Technology Licenciate in telecommunication theory from the Royal Institute of Technology, Stockholm, Sweden. In same year, he joined the Electrical Engineering Department, Eindhoven University of Technology, Eindhoven, The Netherlands, where he received the Ph.D. degree in 1999, and worked as an Assistant Professor until 2006. He is currently a Professor and Head of the Metro-Access and Short Range Communications Group of the Department of Photonics Engineering, Technical University of Denmark.